



UNIVERSIDAD REGIONAL AMAZÓNICA IKIAM

Facultad de Ciencias de la Tierra y Agua

Carrera de Hidrología

Dinámicas espaciales de la minería de oro y sus efectos sobre la pérdida de los bosques tropicales y afectaciones en los recursos hídricos, aplicando sensores remotos: caso de la cuenca alta del Río Napo, Amazonía, Ecuador.

Oscar Enrique Lucas Solis

30 de abril de 2021, ciudad de Tena, Napo, Ecuador

Contenido del documento

CARÁTULA	
DERECHO DE AUTOR.....	ii
CERTIFICADO DEL DIRECTOR	iii
AGRADECIMIENTOS.....	v
DEDICATORIA.....	vi
INDICE GENERAL.....	vii
INDICE DE TABLAS.....	viii
INDICE DE FIGURAS.....	ix
RESUMEN.....	x
ABSTRACT	xi
Spatial dynamics of gold mining and its effects on the loss of tropical forests and water resources affectation, applying remote sensors: case of the upper basin of the Napo River, Amazon, Ecuador.....	1
ANEXOS (Supplementary Materials)	28

Declaración de derecho de autor, autenticidad y responsabilidad

Tena, 30 de abril de 2021

Yo, Oscar Enrique Lucas Solis con documento de identidad N°1314706423, declaro que los resultados obtenidos en la investigación que presento en este documento final, previo a la obtención del título de Ingeniero en Ciencias del Agua son absolutamente inéditos, originales, auténticos y personales.

En virtud de lo cual, el contenido, criterios, opiniones, resultados, análisis, interpretaciones, conclusiones, recomendaciones y todos los demás aspectos vertidos en la presente investigación son de mi autoría y de mi absoluta responsabilidad.

Por la favorable atención a la presente, suscribo de usted,

Atentamente,

Firma:



Oscar Enrique Lucas Solis

Certificado de dirección de trabajo de integración curricular

Certifico que el trabajo de integración curricular titulado: “Dinámicas espaciales de la minería de oro y sus efectos sobre la pérdida de los bosques tropicales y afectaciones en los recursos hídricos, aplicando sensores remotos: caso de la cuenca alta del Río Napo, Amazonía, Ecuador.”, en la modalidad de: proyecto de investigación en formato artículo original, fue realizado por: Oscar Enrique Lucas Solis, bajo mi dirección.

El mismo ha sido revisado en su totalidad y analizado por la herramienta de verificación de similitud de contenido; por lo tanto, cumple con los requisitos teóricos, científicos, técnicos, metodológicos y legales establecidos por la Universidad Regional Amazónica Ikiam, para su entrega y defensa.

Tena, 30 de abril de 2021

Firma:

**MARIANA
VELLOSA
CAPPARELLI**
Assinado de forma digital
por MARIANA VELLOSA
CAPPARELLI
Datos: 2021.05.0219:46:59 -05'00'

.....
Ph.D. Mariana Velloso
C.I: 1758616898

Firma:



Firmado electrónicamente por:
**PABLO ESTEBAN
MENESES JATIVA**

.....
Mgt. Pablo Meneses
C.I: 1714673606

iii



Document Information

Analyzed document	Tesis final - Oscar Lucas.pdf (D103600522)
Submitted	5/3/2021 2:27:00 AM
Submitted by	Mariana
Submitter email	mariana.capparelli@ikiam.edu.ec
Similarity	6%
Analysis address	mariana.capparelli.ikiam@analysis.urkund.com

AGRADECIMIENTOS

Gracias a mis padres por todo su amor y entrega, por apoyar mis decisiones y darme la libertad de cumplir mis sueños y aspiraciones. A mi familia, por hacerme saber siempre lo orgullosos que están de mí y ser mi soporte emocional, afectivo y económico durante toda mi carrera universitaria.

Agradezco a mi tutora Mariana Capparelli, excelente docente, científica y ser humano, por ser una guía en mi camino por la vida, la ciencia y la investigación. A mis docentes, por compartir su conocimiento y experiencia con humildad y mucho amor, sin duda, una parte de ellos y ellas vivirá en mí para siempre. Espero pronto poder compartir con el mundo lo que he aprendido de la misma manera.

Mi agradecimiento también va dirigido a mis amigos de la Universidad, su apoyo, ánimos y cariño han sido combustible para continuar en esta etapa con las dificultades de la emergencia sanitaria.

Gracias al financiamiento de la Unión Europea en coordinación con la Agencia Española de Cooperación Internacional para el Desarrollo (AECID), otorgado a Mariana Velloso Capparelli y Andreu Rico, por permitir desarrollar este proyecto de titulación. Finalmente, agradezco a las instituciones gubernamentales, Ministerio de Ambiente y Agua del Ecuador (MAAE) Dirección Zonal 8, Defensoría del Pueblo del Ecuador (DPE) Delegación Napo y a la Policía Nacional del Ecuador, por su apoyo en la logística de muestreo y protección en las zonas mineras visitadas.

DEDICATORIA

A mis padres, abuelos y hermana.

A mis amigos.

Al Laboratorio virtual de Ecotoxicología del que formo parte.

A mis compañeros de carrera que ven en mi un futuro colega.

A la ciudad donde crecí, Bahía de Caráquez.

A la ciudad de Tena y la provincia de Napo, mi segundo hogar.

INDICE GENERAL

Highlights	1
1. Introduction.....	1
2. Methods	4
2.1. Study area and sampling	4
2.2. LCLU classification and change analysis	5
2.3. Gold mining area change indicators.....	8
2.4. Measurements of physicochemical parameters	9
2.5. Metal analyses.....	9
2.6. Data analysis.....	10
3. Results and discussion	10
3.1. LCLU classification for GM area identification and accuracy assessment	11
3.2. LCLU spatial and temporal trends and change analysis in NRUB.....	12
3.3. Environmental impact of GM sites.....	16
4. Conclusion	18
Acknowledgments	19
Compliance with Ethical Standards	20
Conflict of interest.....	20
References	20
ANEXOS (Supplementary Materials)	28

INDICE DE TABLAS

Table 1. Description of the used geographical database including type, bands, resolution, and the given use.....	7
Table 2. Spectral indices used in LCLU classification. Near Infrared (NIR), short wave infrared (SWIR), Red and Thermal Infrared (TIR) bands.	7
Table 3. Indicators of GM area dynamics.....	9
Table S1. Description of LCLU classes.....	28
Table S2. Location of sampling sites.....	29
Table S3. Overall accuracy and kappa statistics with different data combinations.....	29
Table S4. Accuracy and standard error of user and producer by classes.	30
Table S5. Cross-tabulation matrix between 2015 and 2020 classifications.....	31
Table S6. Changes between 2015 and 2020 classification per land cover class.	31
Table S7. Gold mining area change indicators and water physicochemical parameters....	32
Table S8. Heavy metals concentration in water (μgL^{-1}) and national and international normatives.....	33
Table S9. Heavy metals concentration in sediment (μgg^{-1}) and national and international normatives.....	34

INDICE DE FIGURAS

Figure 1. Study area. Optical satellite image composite of the Napo River Upper Basin in the Ecuadorian Amazonia.....	5
Figure 2. Methods. A) Flowchart of data processing. B) Minimum points used for LCLU classification in all years. High density vegetation (HDV), Low density vegetation (LDV), Riparian zone (RZ), Anthropogenic zone (AZ), Bare soil (BS), Gold mining (GM) and Non observed (NO).....	6
Figure 3. LCLU classification for A) 2015 and B) 2020. Example areas where GM area change can be observed for C) 2015 and D) 2020. High density vegetation (HDV), Low density vegetation (LDV), Riparian zone (RZ), Anthropogenic zone (AZ), Bare soil (BS), Gold mining (GM) and Non observed (NO).....	12
Figure 4. Evolution of LCLU classes from 2015 to 2020 in study area percentage. A) High density vegetation B) Low density vegetation C) Riparian zone D) Anthropogenic zone E) Bare soil and F) Gold mining.	13
Figure 5. GM extent for the whole study area from 2015 to 2020, along national gold production from 2015 - 2019 (data for 2020 was not available yet; BCE, 2021), national gold exportation from 2015 to 2020 (BCE, 2021) and international gold price (World Gold Council, 2020).	15
Figure 6. PCA analysis for water and sediment. Dim1 and Dim2 axes are the first two principal components. Results of hierarchical cluster analysis for water and sediment are under its respective PCA plot. Sampling point location area shown in Figure 1 and its coordinates in Table S2.	18
Figure S1. Gold mining land covers evolution from 2015 to 2020 in an example area. The background is a Sentinel-2A image for 2020.....	30

RESUMEN

Los impactos de la minería de oro (MO) son devastadores, incluido el cambio de paisajey la deforestación, la pérdida de servicios ecosistémicos y especies nativas, la reducción de la calidad del agua y la contaminación del suelo y el aire. El rápido aumento de esta actividad en la cuenca del Amazonas, la escasez de estudios, la difícil detección de impactos y el monitoreo requieren técnicas integradas que puedan evaluar los impactos de la MO en este importante ecosistema. Este estudio busca utilizar una técnica de teledetección para evaluar la dinámica de cambios de cobertura y uso de la tierra y los impactos derivados de la actividad de MO durante un período de 6 años en la Amazonía ecuatoriana y asociarlos con datos auxiliares de calidad de agua y contaminación por metales en agua y sedimentos para comprender el grado de contaminación y sus riesgos para la salud ambiental. La MO duplicó su extensión de 0.15% (651 ha) a 0.30% (1317 ha) del área total de estudio, degradando áreas principalmente boscosas. La asociación de información ha hecho posible evaluar el impacto de la MO de manera integradora en 9 sitios, mostrando que los sitios con un rápido aumento de su extensión y degradación del paisaje tienen un efecto directo sobre la contaminación por metales en agua y en los parámetros fisicoquímicos, mientras que los lugares con menor incremento tienen mayor ocurrencia de metales en sedimentos y mayor cambio en su ubicación que en su extensión.

Palabras clave: Minería de Oro, cambio de cobertura y uso del suelo, sensores remotos, Amazonía, Google Earth Engine.

ABSTRACT

Gold mining (GM) impacts are devastating, including landscape change and deforestation, loss of ecosystem services and native species, contribution of carbon emission and sediment loads, reduced water quality, and soil and air contamination. The rapid increase in this activity across the Amazon basin, the scarcity of studies, the difficult detection of impacts and monitoring require integrated techniques that can assess the impact of GM on this important ecosystem. Google Earth Engine (GEE) is a useful tool for evaluating anthropic activities incidence on the dynamics of planetary coverage. Thus, this study seeks to use a remote sensing technique in GEE to assess land cover and land use changes dynamics and impacts derived from GM activity over a 6-year period in the Ecuadorian Amazon and to associate them with quality auxiliary data water and metal contamination in water and sediment to understand the degree of contamination and its risks to environmental health. GM doubled its extent from 0.15% (651 ha) to 0.30% (1317 ha) of the total study area, degrading mainly forested areas and leaving heterogeneous landscapes covered by grassy or bare soils. The combination of GM area change indicators with environmental quality data has made it possible to assess the mining activity impact in an integrative way in 9 GM sites, showing that sites with rapid increase of its extent and landscape degradation have a direct effect on metal contamination in water and physicochemical parameters, while places with lower increase have a higher occurrence of metals in sediments and a greater change in its location than in its extension.

Key words: Gold Mining, land cover and land use change, remote sensing, Amazon, Google Earth Engine.

- La revista a la cual someteré mi artículo es **Science of the Total Environment**

Spatial dynamics of gold mining and its effects on the loss of tropical forests and water resources affectation, applying remote sensors: case of the upper basin of the Napo River, Amazonia, Ecuador.

Oscar Lucas-Solis¹

1. Facultad de Ciencias de La Tierra y Agua, Universidad Regional Amazónica Ikiam, Km 7 Vía Muyuna, Tena, Napo, Ecuador

Highlights

- Remote sensors have made it possible to identify and delimit gold mining areas and their change over time.
- Gold mining has doubled in extent from 2015 to 2020 in the upper Napo River basin.
- Gold mining has short- and long-term environmental quality effects and these can be analyzed by integrating remote sensing with in situ environmental data.

1. Introduction

The Amazon basin is a world biodiversity hotspot that provides diverse ecosystem services, for instance, global climate regulation and water provision for local communities (Delgado-Aguilar, Konold, & Schmitt, 2017). This region also has a dense river network that drains one of the most forested areas on Earth, from the Andes to the Amazon floodplain and its outlet in the Atlantic Ocean. However, anthropogenic activities such as gold mining (GM), oil extraction, agriculture, livestock, hydroelectric dams, and road construction, pose a risk to the health of this relevant and vulnerable freshwater ecosystem (Alexiades, Encalada, Lessmann, & Guayasamin, 2019; Capparelli et al., 2020; Galarza et al., 2021). Deforestation rates in the Amazon are associated primarily with agriculture, ranching, logging, and fire, but GM activities are also responsible for a large fraction of forest loss and disturbance (Potapov et al., 2017). Important GM activities started in the 1950's and currently, hundreds of thousands of people are directly involved in it due to the relatively high rise in gold prices and local government support in countries like Brazil, Peru and Ecuador in the last few years (Lobo, Costa, Novo, & Telmer, 2016; Vela-Almeida, 2018; World Gold Council, 2021).

In the developing countries of South America, Africa and Asia, artisanal and small-scale are the main types of GM practice (Lobo et al., 2016). Artisanal GM is characterized

by making use of tools and simple and portable machines by individuals, families, or communities, while the categorization of industrialized GM (i.e. small, medium, large) varies by reason of the area of the concessions, volume of processing and production, amount of investments and technological conditions, but it is characterized by the use of heavy machinery (Ministerio del Ambiente y Agua, 2020b). GM impacts are severe compared to the other deforestation drivers, leaving a highly altered landscape, ecosystem services loss, water quality reduction and mercury contamination of water, soil and air, loss of native species, sediment loads, increased mortality in adjacent tropical forests, and carbon emissions from deforestation (Asner, Llacayo, Tupayachi, & Luna, 2013; Caballero Espejo et al., 2018). Those impacts increase with socioeconomic factors such as poverty, infrastructure, and illegal capital flow (Adler Miserendino et al., 2013). Land cover and landscape after GM activity are constituted of extensive areas of bare soil, sediment-laden ponds, and remnant or new vegetation (Caballero Espejo et al., 2018). These areas have a poorer regeneration potential compared to areas with different pressures like agriculture, due to the fact that soils after GM activity lose their structure with a high sand content and decreases their fertility with a low organic matter content and low cation exchange capacity (Román-Dañobeytia et al., 2015).

Artisanal and small-scale GM in the Amazon could have severe negative environmental issues and social impacts on the population surrounding the mining projects because these are set near rivers and streams due to the conditions (i.e. placer and paleoplacer deposits) where gold is found in the area (Adler Miserendino et al., 2013; Agencia de Regulación y Control del Agua (ARCOM), 2019). Profits from GM could subserve the Amazon region to alleviate poverty, basic services and water security deficiencies, but that suppose native flora and fauna loss, contamination of water resources, soil and air, which also translates into economic losses in agriculture, fisheries, soil productivity, and tourism (Secretaría Nacional de Planificación y Desarrollo (SENPLADES), 2015; Adler Miserendino et al., 2013; Villa-Achupallas, Rosado, Aguilar, & Galindo-Riaño, 2018). The main concern with GM is that its short-term benefits to the state will not compensate for the permanent ecosystem damage, and long-term economic and ecosystem services affectation at the local and regional level (B. Roy et al., 2018). As happened with oil exploitation, which implied a 44% primary forest reduction, loss of biodiversity and negative effects on human health in the Ecuadorian Amazonia (Barraza et al., 2018).

Environmental impact assessment and monitoring should be an integral part of GM operations because they can be used for long-term environmental management, as well as to know the recovery and rehabilitation of GM areas (Charou, Stefouli, Dimitrakopoulos, Vasiliou, & Mavrantza, 2010). GM areas in the Amazon usually are difficult to access or even dangerous by illegal activities (Elmes, Ipanaqué, Rogan, Cuba, & Bebbington, 2014). The exact location and evolution of the expansion of GM are difficult to evaluate or monitor accurately (Asner et al., 2013). For that reason, researchers have chosen to evaluate and monitor the tropical forest degradation by GM progress using remote sensing in other areas of Latin America like the Peruvian or Brazilian Amazonia (Anaya et al., 2020; Asner & Tupayachi, 2017; Caballero Espejo et al., 2018; Lobo et al., 2016). One of the tools that has gained great relevance for monitoring, tracking, and managing the Earth's environment and resources is Google Earth Engine (GEE) which is a portal that provides free access to satellite and ancillary data, cloud computing, and algorithms for processing large amounts of data (Kumar & Mutanga, 2018). Remote sensing applications are diverse, for instance, in the Peruvian Amazonia, GM impacted areas monitoring combined with water quality information were key to understand land cover and land use (LCLU) change, water resources deterioration, and social and environmental impacts (Asner et al., 2013; Elmes et al., 2014; Lobo et al., 2016). These types of impacts could not be evaluated with water quality monitoring alone, since these give an idea of the state of water resources at a certain time, but these can also be affected by other social and economic factors (Lobo et al., 2016).

Historically, the ecosystems on the eastern Andes of Ecuador, at the transitions with Amazonia, have been largely impacted by mining activities (Capparelli et al., 2020; Perez, 2015). Recently, the national territory of Ecuador destined for GM exploration and future exploitation drastically increased from 3% to 13% spread across the country, including many forests designated as "protected" (B. A. Roy et al., 2018). This increases concern in areas where GM is still incipient but is already having impacts on water quality and generating risks for human and environmental health., such as the Napo River upper basin (NRUB) (Capparelli et al., 2020; Galarza et al., 2021; Jiménez-Oyola et al., 2021). Even though artisanal mining (i.e. mining without heavy machinery and granted to small companies or local communities) is the most common concession authorized, industrial mining represents 98% of the total territory for the exploitation of gold at the Napo province (33,718 ha). Few risk assessments have been carried out in streams of this area using multiple lines of evidence that reported a low aquatic ecosystem quality, as well as

high human health risk (Capparelli et al., 2020; Galarza et al., 2021; Jiménez-Oyola et al., 2021). These conclusions were based mainly on the elevated presence of potentially toxic elements such as Cd, Cu, Pb, and other metals in both water and sediments, but also macroinvertebrates absent which is a biological indicator of bad water quality, and bioassays with *L. sativa* that indicated water and sediment sample phytotoxicity related to GM activity (Capparelli et al., 2020; Galarza et al., 2021).

In the Ecuadorian Amazonia, remote sensing has been used to monitor mountain humid forests, suspended sediment yield, and anthropogenic disturbance mapping, but relating GM activity as a factor of change in LCLU and/or landscape in the Ecuadorian Amazonia is still lacking (Goerner, Gloaguen, & Makeschin, 2007; Keating, 1997; Santos, Meneses, & Hostert, 2019; Tarras-Wahlberg & Lane, 2003). Despite the rapid increase in this activity in the NRUB and the entire Amazonia, its biological and hydrological importance, and the consequences for neighboring populations and communities, ecosystems and water and aquatic resources (Asner et al., 2013; Asner & Tupayachi, 2017; Brooks et al., 2006; Elmes et al., 2014). Therefore, this study seeks to (1) use a remote sensing technique to assess the dynamics and impacts in LCLU change derived from GM activity in a 6-year period in the NRUB, a vulnerable and biodiverse tropical landscape, and (2) associate them with ancillary data of gold price, national production and exportation, water quality and metal contamination in water and sediment to understand the contamination degree and its risks to environmental health.

2. Methods

2.1. Study area and sampling

The Napo River is one of the main tributaries of the Amazon River, having a large number of natural resources and its landscapes range from the Andean foothills to the Amazon plain (Gobierno Autónomo Descentralizado Provincial de Napo (GADP Napo), 2014). NRUB is home to about 116,700 inhabitants and has an area of approximately 445595 ha (Gobierno Autónomo Descentralizado Provincial de Napo (GADP Napo), 2018; Instituto Nacional de Estadística y Censos (INEC), 2010). The region of the sub-Andean mountain ranges in the Napo province hosts important gold prospects, with deposits of the placer and paleoplacer type, which is why alluvial gold mining has occurred since colonial times on the banks of the Napo River (Carranco, 2017; Gobierno Autónomo Descentralizado Provincial de Napo (GADP Napo), 2014).

The NRUB is a humid tropical zone with abundant rainfall (up to 4400 mm/year in

the south and east) and a high density of rivers and streams (Bravo-Medina et al., 2017; Prefectura de Napo, 2015) (Figure 1). The study area covers the southern Napo province, where gold mining concessions are concentrated to the south in the Anzu, Jatunyacu, and Napo river basins (formed from the union of the two previous ones), being these highly threatened by mining activity. NRUB land is covered by native forest (60.87%), agricultural land (36.30%), water bodies (1.88%), anthropic zone (0.72%), shrub and herbaceous vegetation (0.05%), and others (0.18%) (Hurtado Pidal, 2014; Ministerio del Ambiente y Agua, 2020a). There is a high concentration of towns, especially on the riverbanks, in addition to three of the most populated cantonal heads, Tena, Archidona, and Carlos Julio Arosemena Tola.

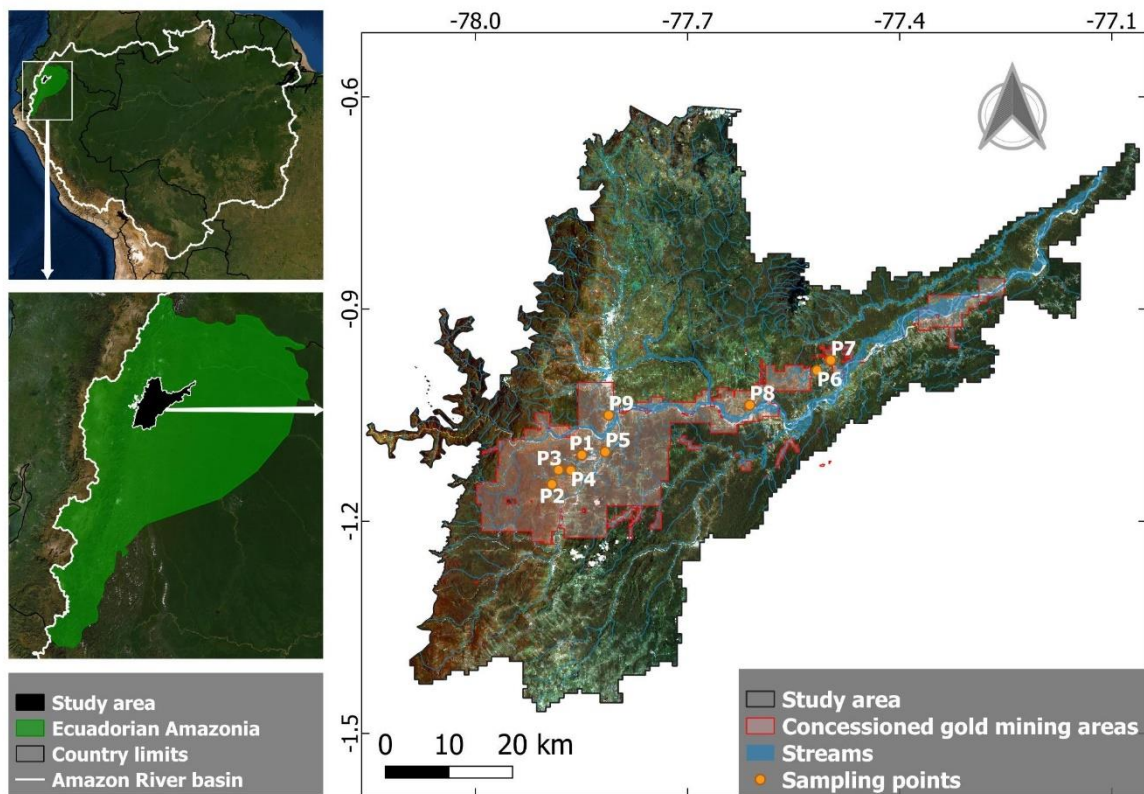


Figure 1. Study area. Optical satellite image composite of the Napo River Upper Basin in the Ecuadorian Amazonia.

2.2. LCLU classification and change analysis

The methods used in this research for LCLU classification are summarized in a flowchart (Figure 2A). On the other hand, the data used for the classification and their descriptions are in Table 1. The first step consists of the building of six yearly GEE cloud and shadow masked composites from 2015 to 2020, which include Landsat 7 ETM+ (Enhanced Thematic Mapper Plus), Landsat 8 OLI-TIRS (Operational Land Imager -

Thermal Infrared Sensors), and Sentinel-1A atmospheric and orthorectified corrected surface reflection image collections. Each image collection was filtered by date (a whole year) and clipped with a shapefile of the study area, also optical image collections were cloud and shadow masked (Anaya et al., 2020). The bands used in the classification are in Table 1 for both optical and SAR image collections. Landsat 7 ETM+ images present gaps in the image since 2007, for that reason a method to fill those gaps was performed, which consisted in using a 8 x 8 pixels focal mean function (Coulter et al., 2016). Due to the prevalence of clouds in the tropical forest and to reduce the speckle of SAR images while removing noise (extreme backscattering values), it was necessary to statistically reduce the image collections to one single image, calculating the median of the pixels peryear (Souza et al., 2020). Digital elevation model (DEM) data from Shuttle Radar Topography Mission (SRTM) available in GEE and a raster containing distance from rivers (DFR) derived from a shapefile of streams the Ecuadorian Geographic Military Institute were added to the composites and also used in classification (Anaya et al., 2020). The next step was the indices calculation from Landsat 7 ETM+ and 8 OLI image collections since they have been used to improve the classification accuracy (Capolupo, Monterisi, & Tarantino, 2020). All of the calculated spectral indices are presented in Table 2.

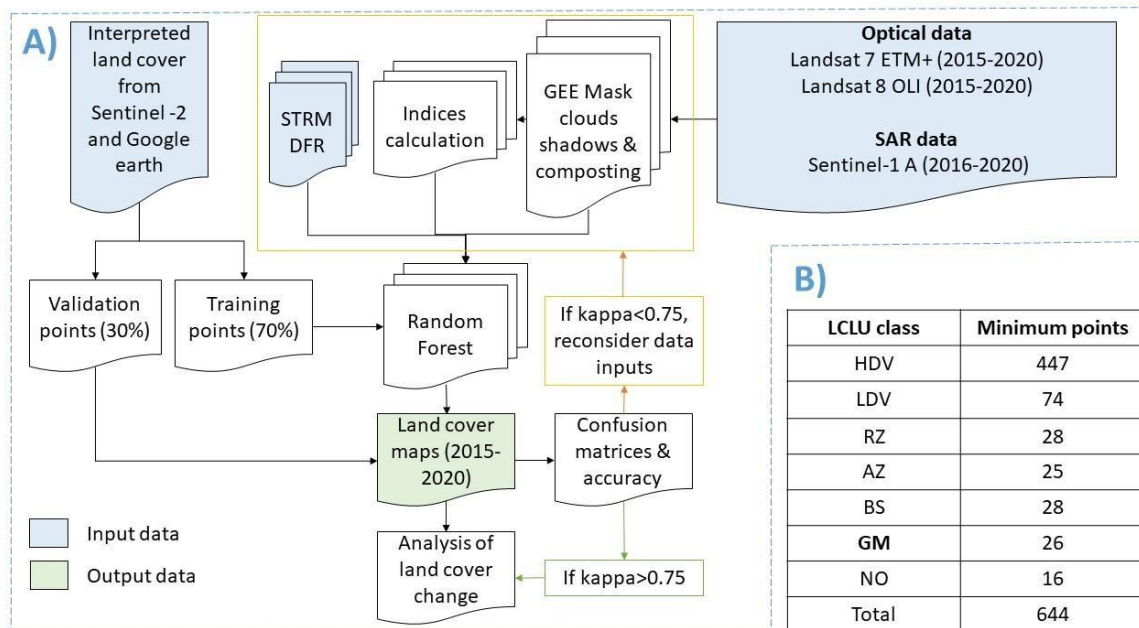


Figure 2. Methods. A) Flowchart of data processing. B) Minimum points used for LCLU classification in all years. High density vegetation (HDV), Low density vegetation (LDV), Riparian zone (RZ), Anthropic zone (AZ), Bare soil (BS), Gold mining (GM) and Non observed (NO).

Table 1. Description of the used geographical database including type, bands, resolution, and the given use.

Image collection	Type	Bands	Resolution	Use
Landsat 7 ETM+	Optical	B1, B2, B3, B4, B5, and B7	30 m	Classification input data
Landsat 8 OLI	Optical	B2, B3, B4, B5, B6, and B7	30 m	Classification input data
Sentinel 1 A	SAR	VH and VV polarization	10 m	Classification input data
Sentinel-2A MSI	Optical	B2, B3, B4, and B8	10 m	Training and validation data
STRM	DEM	SRTM	30 m	Classification input data
DFR	Distance	DFR	10 m	Classification input data

Table 2. Spectral indices used in LCLU classification. Near Infrared (NIR), short wave infrared (SWIR), Red and Thermal Infrared (TIR) bands.

Spectral index	Equation
Normalized Difference Vegetation Index (NDVI)	$NDVI = \frac{NIR - Red}{NIR + Red}$
STRed index	$STRed\ index = \frac{SWIR1 + Red - TIR1}{SWIR1 + Red + TIR1}$
Normalized Difference Bareness Index (version 2) (NDBaI2)	$NDBaI2 = \frac{SWIR1 - TIR1}{SWIR1 + TIR1}$

In QGIS, 500 random sampling points were distributed in all extensions of the study area. Yearly Sentinel-2A MSI (MultiSpectral Instrument) image collections available in GEE and google earth images were used for the interpretation of LCLU points. Nine LCLU classes were assigned to improve the classification (Table S1); however, the final LCLU classes were reclassified into six and they are shown in Figure 2B. LCLU classes were High density vegetation (HDV), Low density vegetation (LDV), Riparian zone (RZ), Anthropogenic zone (AZ), Bare soil (BS), and Gold mining (GM) which are more detailed in Table S1. Since most of the coverage is HDV or forested areas, additional points were established up to at least 25 points per LCLU class (Figure 2B). 70% of those points were destined for training the algorithm or classifier, and the remaining 30% for validation. The machine-learning algorithm for supervised LCLU classification used was Random Forest with 500 decision trees (Anaya et al., 2020; Belgiu & Drăgu, 2016; Souza et al., 2020). After training the algorithm for each year, the classification was performed and validated. Several combinations of input data were performed and the one with the highest average overall accuracy and kappa index was chosen. The classification was approved when the kappa index was equal to or above 0,75, which represents a moderate agreement (Caballero Espejo et al., 2018).

Finally, to evaluate LCLU changes between 2015 and 2020, the results of the classification for those years were generally compared through a cross-tabulation matrix, which helps to evaluate the net change and the interchange as well as the gross losses and gains (Pontius & Santacruz, 2014). LCLU change by each class was also performed to identify the individual loss and gain area. This procedure and the reclassification were performed in R software, where the pixels affected with cloud and shadow even in only one year were excluded from the analysis (R Core Team, 2017).

2.3. Gold mining area change indicators

Nine sites located downstream areas directly affected by industrial-size mining were sampled in December of 2020, in order to evaluate physicochemical parameters, metal contamination in water and sediment, and relate them to GM area change indicators. All the sites were located within gold mining concession territories (Figure 1, Table S2). Surface water (100 mL) and sediment (150 g) samples were taken; water samples were acidified (to pH 2) in the field with HCl for metal analysis. Bottles for water were rinsed thrice with the samples and sediments were collected with a plastic hand trowel and stored in plastic bags.

Once the GM areas had been identified and delimited through the supervised classification in the NRUB, the affected areas for the 9 sampling sites for each year from 2015 to 2020 and for the 6-year period by overlapping them. Then those areas were measured using QGIS 3.10.14 (QGIS Development Team, 2021). In order to know the affected areas over the whole 6-year period, the overlapping was necessary due to the fast GM dynamics in which it can move to other LCLU classes like HDV and BS but maintaining the effects of GM activity on water quality and soil fertility (Caballero Espejo et al., 2018; Román-Dañobeytia et al., 2015). In addition, the affected area of each site in 2015 and 2020 were used to compare whether the areas were increasing or decreasing and to see how they interfere with the water parameters and the concentration of metals in the water and sediments. This was calculated through the percentage of area currently affected with respect to the GM area in 2015 and with the 6-year period impacted area (Table 3).

Table 3. Indicators of GM area dynamics.

GM area change indicators	Equation
GM area change from 2015 to 2020 (AC, %)	$AC = \frac{GM\ area\ 2020}{GM\ area\ 2015} * 100$
Portion of GM affected area in 2020 respect to the 6-year period (AP, %)	$AP = \frac{GM\ area\ 2020}{GM\ area\ 6 - year\ period} * 100$

2.4. Measurements of physicochemical parameters

Conductivity, pH, oxidation reduction potential (ORP), total dissolved solids (TDS) and dissolved oxygen (DO) were measured in situ using a professional plus multiparameter. Turbidity was also measured in situ with a HACH 2100 Q turbidimeter. The equipment was previously calibrated with standard solutions. In the laboratory, dissolved organic carbon (DOC) concentrations were measured using a total organic carbon analyzer (TOC-L Shimadzu, Japan). The total suspended solids (TSS) were analyzed according to APHA (2018).

2.5. Metal analyses

Metals (As, Cd, Co, Cr, Cu, Ni, Pb and Zn) analysis in water and sediment samples were performed at the Laboratory of the University of Cuenca, Ecuador after acid digestion using 8 ml of ultra-pure nitric acid and 2 ml of hydrochloric acid (Merck trend). The samples were analyzed using a Perkin Elmer 350X ICP-MS. For the reading of

metallic analytes, an adaptation of Method 200.8 EPA (United States Environmental Protection Agency) was used (United States Environmental Protection Agency (US EPA), 2014). Calibration curves were created from a multi-element standard Inorganic Venture, at concentration from 0.1 to 0.0005 mg L⁻¹. Quality control for trace elements analysis was implemented using certified reference water (CRM 1640a) and sediment (CRM 1646a) (NIST, Gaithersburg, Maryland) every 10 samples, as well as at the beginning and at the end of each sample batch. Recovery percentages were calculated to determine possible matrix effects and method accuracy. All trace metal concentrations were corrected based on the recovery percentages obtained in each analysis, which ranged from 91% to 100% for water, and 69% to 93% for sediments.

2.6. Data analysis

National legislation (TULSMA, Ministerio del Ambiente, 2015), the Environmental Protection Agency of the United States (United States Environmental Protection Agency (US EPA), 1996) and the Environmental Quality Guidelines of Canada (Canadian Council of Ministers of the Environment (CCME), 2002), were contrasted with metal concentrations in water samples. The CCME (2002) and national legislation (TULSMA, Ministerio del Ambiente de Ecuador, 2015) of stream sediments and soil quality standard, respectively, were used for sediment samples. Those comparisons allow to know if metals concentrations can have negative effects on aquatic life (Long, Macdonald, Smith, & Calder, 1995).

Principal Component Analysis (PCA) was used to summarize LCLU change data, physicochemical parameters of water samples and As, Cd, Co, Cr, Cu, Ni, Pb and Zn concentrations in water and sediments samples. All variables were normalized by z-score normalization. The first two principal components (PCs) were investigated and their correlations to each variable were tested through the Pearson's correlation test.

Hierarchical cluster analyses were used to assess the presence of natural clusters among sampling sites by an iterative process that defined clusters based on the (dis)similarities of two sites. Dissimilarities between sites were calculated by Euclidean distances for normalized variables; the Group Average Link was used as the agglomeration method in the classification. All statistical analyses were performed using the R software (R Core Team, 2017).

3. Results and discussion

3.1. LCLU classification for GM area identification and accuracy assessment

Six annual LCLU maps for NRUB with supervised classification from 2015 to 2020 using Google Earth Engine at 30 m pixel resolution were generated, using multisource data. A combination of optical and Synthetic Aperture Radar (SAR) satellite data such as Landsat and Sentinel-1 collections have been shown a great performance in identifying land use and land cover changes, especially in tropical forest landscapes where high cloud cover is the main concern (Anaya et al., 2020; De Alban, Connette, Oswald, & Webb, 2018). The combination of inputs used for classification in this study that had the highest average overall accuracy and kappa index (88.5% and 0.818, respectively) for the 6-year period was optical and SAR image collection, indices derived from them (NDVI, NDBaI2 and STRedindex) and the terrain information (DEM, and DFR) (Table S3). NDBaI2 has been shown to be useful in classifying mining, water, urban area, HDV and LDV, while STRedindex index just mining, water, HDV and LDV (Capolupo et al., 2020). The standard error of the overall accuracy was less than 1%, which means that it did not vary over the time series from 2015 to 2020. On the other hand, the combination with the lowest performance was optical image collection and DFR with an overall accuracy of 86.9% and a kappa index of 0.787.

The user and producer accuracy estimates were summarized by averaging them over the 6 years timespan of this study (Table S4). This allowed to break down the overall accuracy for the NRUB into LCLU class levels. LCLU classes user accuracies from highest to lowest were NO (97.62%), AZ, RZ, HDV, GM (89.53%), beaches, LDV, BS and roads (49.94%). The lower user accuracy in roads may be related to their small width with respect to the spatial resolution of the classification, which is 30 m and generates spectral mixture (Song, 2004). Producer accuracies from highest to lowest were HDV (98.34%), beaches, RZ, NO, roads, AZ, GM (77.67%), LDV, and BS (47.71%). The highest standard error value for user accuracy was 8.33% in BS and for producer accuracy was the same percentage in NO, denoting high variability in the 6-year period. The LCLU class with the worst overall accuracy was BS. The lower accuracy and precision of BS could have consequences in GM classification since GM operations can also result in barren lands after vegetation removal and generate confusion or misclassification (Anaya et al., 2020). In Figure 3, LCLU classification for 2015 (a) and 2020 (b) are shown and in the example areas for these years (c and d) a misclassification of AZ (black) can be appreciated around GM (red) sites and also GM (red) is misclassified near RZ (light blue).

This can be explained by the similarity of the spectral signature that mining has with anthropic zones and riparian zones, which STRedindex that was included helps to differentiate (Capolupo et al., 2020). The GM area change for the same example area from 2015 to 2020 can be appreciated in Figure S1.

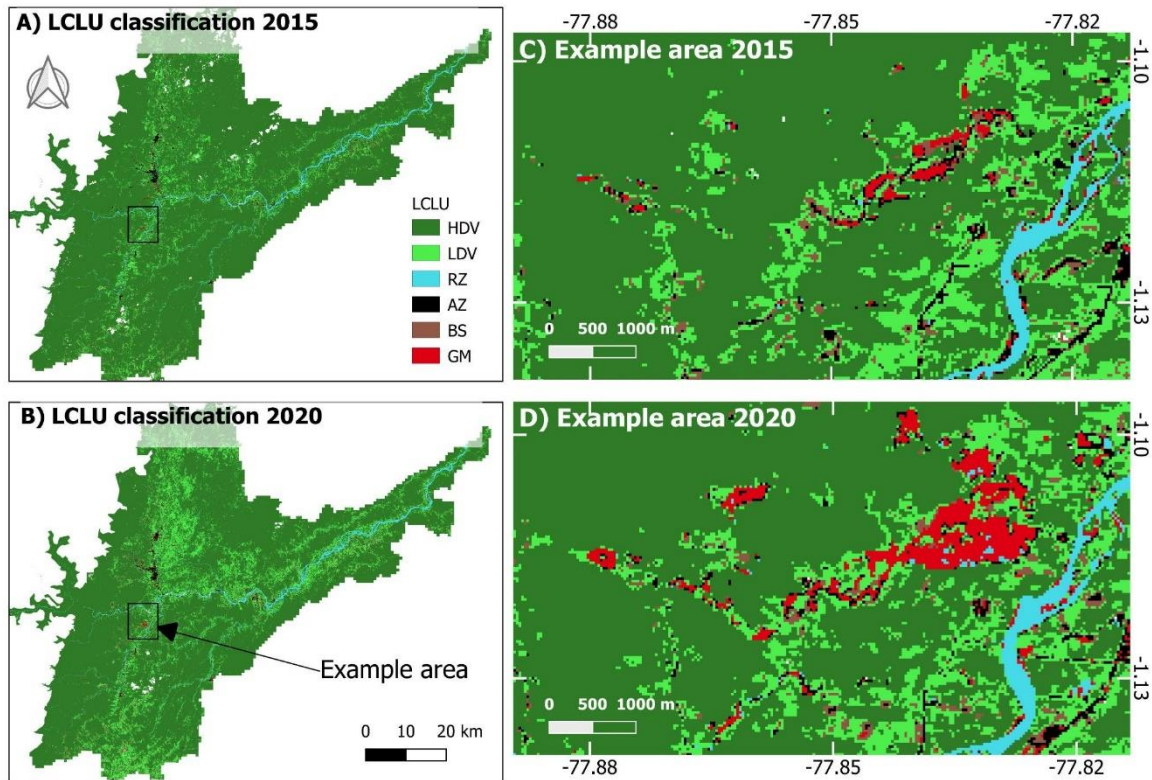


Figure 3. LCLU classification for A) 2015 and B) 2020. Example areas where GM area change can be observed for C) 2015 and D) 2020. High density vegetation (HDV), Low density vegetation (LDV), Riparian zone (RZ), Anthropic zone (AZ), Bare soil (BS), Gold mining (GM) and Non observed (NO).

3.2. LCLU spatial and temporal trends and change analysis in NRUB

Temporal trends of the six studied LCLU classes including HDV, LDV, RZ, AZ, BS and GM area from 2015 to 2020 are presented in Figure 4. In 2015, the HDV class covered 87.12% of the NRUB, with 388224 ha while LDV covered 8.78% with 39158 ha. The remaining LCLU classes represented 1.34% (6008 ha) for RZ, 1.08% (4831 ha) for AZ, 1.50% (6721 ha) for BS and 0.14% (651 ha) for GM. In 2020, the HDV class was reduced to 78.87% of NRUB, with 351449 ha while LDV increased to almost double 16.16% with 72025 ha. RZ, AZ, BS and GM classes reached 1.48% (6605 ha), 1.21% (5378 ha), 1.97% (8820 ha) and 0.29% (1316 ha), respectively. GM class was the one which doubled its extent in the 6-year period, followed by LDV which increased in 1.8

times, RZ had a minimum change (almost 1:1 ratio) and HDV class was the only one which decreased.

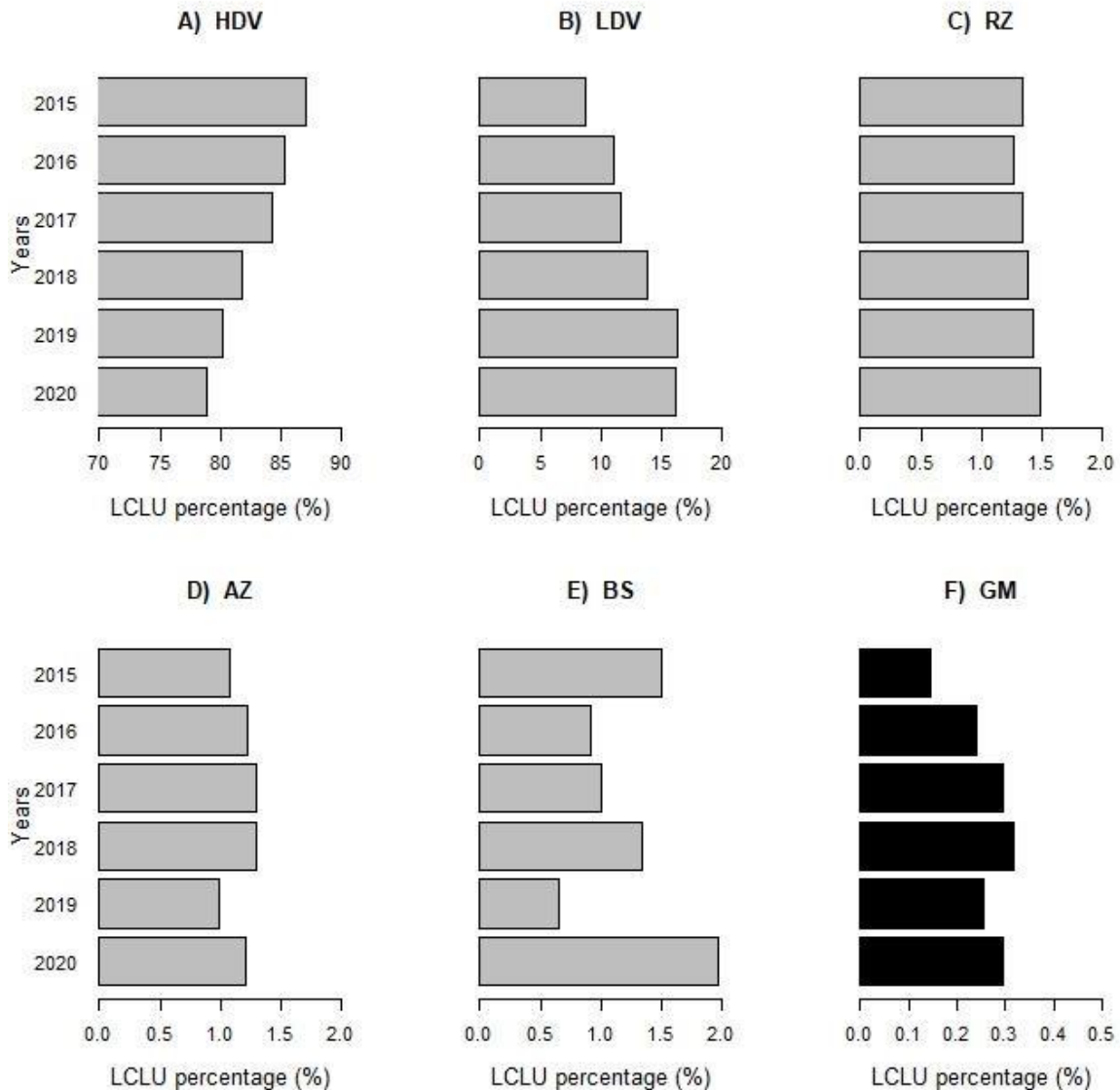


Figure 4. Evolution of LCLU classes from 2015 to 2020 in study area percentage. A) High density vegetation B) Low density vegetation C) Riparian zone D) Anthropic zone E) Bare soil and F) Gold mining.

In the Ecuadorian Amazonia, the presence of mining began about 50 years ago in the south and nowadays, the most important large-scale gold exploitation projects are settled there becoming an important income source as well as a disturbing contamination source (Adler Miserendino et al., 2013). However, those large-scale GM projects just began to occur in 2020, so before that, 100% of GM in the country was artisanal (22%) and small-scale (78%). Contrary to the international scenario where 82% of production is attributed to large-scale projects, 10% to medium-scale and only 8% to artisanal and small-

scale GM (Banco Central del Ecuador (BCE), 2017). Gold mining in NRUB is still rising (~0.7% of national gold production) compared to other areas in the country, since currently a larger amount of gold production (84.3%) clearly comes from small and artisanal GM in the Oro, Azuay, Zamora Chinchipe, and Imbabura provinces (Larenas, Fierro, & Fierro, 2017; Ministerio del Ambiente y Agua, 2020b). In the NRUB, gold exploitation concessions have reached the number of 152 distributed along the Napo river tributaries, being almost 60% for artisanal GM, leaving the remainder for industrial GM in small and medium scales (Ministerio del Ambiente y Agua, 2020b). Larger-scale GM areas play a secondary role compared to small-scale and artisanal; the latter are determinants of the patterns and rate of degradation of highly biodiverse tropical forests (Asner et al., 2013). Thus, the large number of artisanal GM concessions and the extensive area of industrial mining concessions (98,3% of the total area) may pose a risk in the NRUB land degradation.

In order to analyze a relation between spatio-temporal extent of GM with national gold production and exportation and international gold price, Figure 5 was generated. GM areas and gold price have increased along the 6-year period from 651 to 1317 ha and 1158 to 1774 USD/Onz, respectively. National gold mining production decreased from 7723 to 6293 kg and gold exportation from 20801 to 7283 kg, showing a weak rise in 2018 for production and 2019 for exportation. The year with highest national gold production matches the year with the highest GM extent in NRUB, but this is not a clear relation due to the gold production value is at national scale. However, GM areas have shown to increase like the gold price. If the values of the export of Gold from Ecuador are compared with the production values in 2015, the great difference between these variables is evident, which would be explained by the illegality and informality of artisanal and small-scale mining (Banco Central del Ecuador (BCE), 2017). A special regime regulation for small mining and artisanal mining was promulgated in November 2009 due to the relevance of these mining types (Frækaland Vangnes, 2018). The Ministry of Mining and these regulations, position small mining and artisanal mining as a priority for the economic development of the country and together with medium and large-scale mining are administered, regulated, controlled and managed by the institutional structure that defines the Law (Adler Miserendino et al., 2013). Since 2016 the export and production values are more similar, which shows the effort of Mining Regulation and Control Agency (ARCOM) in the containment of illegal mining and smuggling, mainly to Peru (Agencia de Regulación y Control del Agua (ARCOM), 2018; Banco Central del Ecuador (BCE),

2020). The actions of ARCOM could also influence the reduction of the mining area in 2019 (Figure 5).

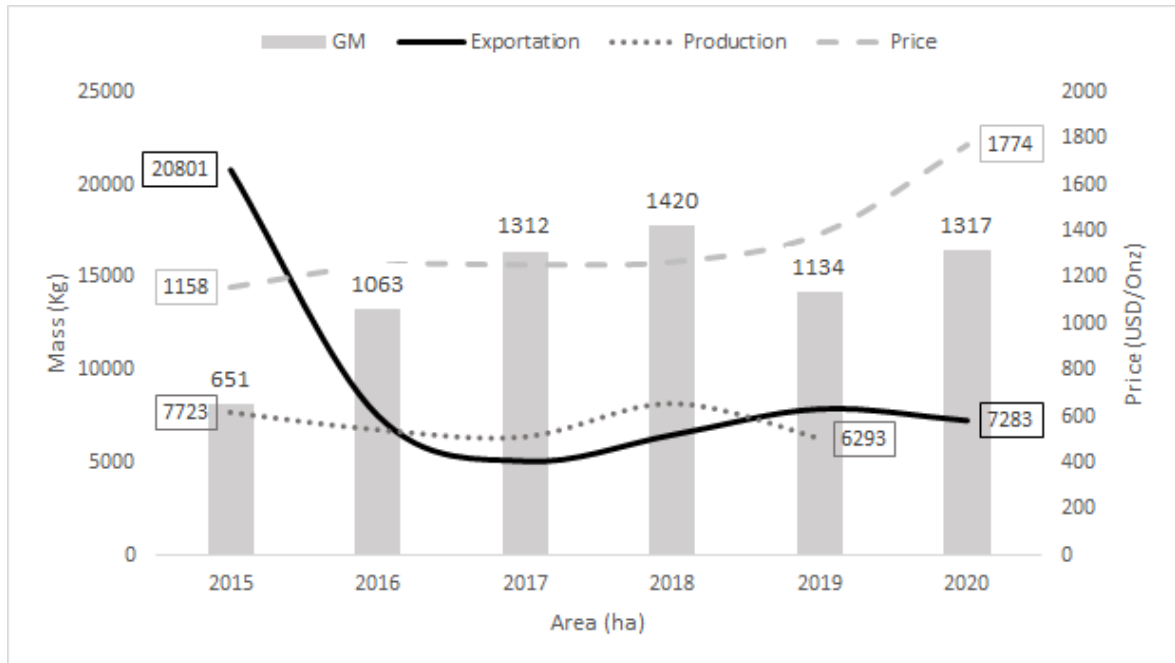


Figure 5. GM extent for the whole study area from 2015 to 2020, along national gold production from 2015 - 2019 (data for 2020 was not available yet; BCE, 2021), national gold exportation from 2015 to 2020 (BCE, 2021) and international gold price (World Gold Council, 2020).

For the LCLU change analysis, a cross-tabulation matrix between 2015 and 2020 classifications can be found in Table S5 and information about the change per each class is in Table S6. Table S5 shows that HDV for 2015 was the LCLU class that transitioned the most for 2020 principally to LDV and BS. That transition could be associated with agricultural activities and GM which are the main drivers that leave LDV and BS as a result (Souza et al., 2020). GM was the LCLU that transitioned the least from 2015 to 2020, and it passed mainly to AZ and LDV. The LCLU classes which transitioned the most to GM were AZ and HDV, followed by RZ, LDV and BS. The leading of AZ may be influenced by the misclassification of GM in AZ discussed in section 3.3.1, but HDV may suggest deforestation (HDV) due to GM activities, which has been also discussed by other authors in the Amazon basin (Anaya et al., 2020; Asner et al., 2013; Asner & Tupayachi, 2017; Caballero Espejo et al., 2018). LDV was the class that most of the other classes transitioned to, while RZ is the one that became the least. Most anthropic activities result in BS and LDV, especially GM, which has a very heterogeneous landscape after its operations (Caballero Espejo et al., 2018). From Table S6, it is observed that HDV was the

LCLU that lost more of its extent (~36.775 ha), while LDV, AZ, BS and GM (~665 ha) are gaining area in the NRUB. RZ showed more persistence than gain or loss. The overall change of LCLU in the NRUB was 15.57% of its territory, 7.78% were quantity changes which refers to changes from one class directly to another and 7.80% were allocation changes. Allocation changes were 7.45% of exchange and 0.34% of shift which refers to spatial distribution of the transitions. HDV and LDV had more quantity changes and RZ, AZ, BS and GM had more exchange. The last two are the most dynamic in terms of transition and their changing rate is irregular (Lobo et al., 2016). BS had the highest shift changes, HDV and GM had no shift changes.

3.3. Environmental impact of GM sites

The evaluation of the impact of GM activities in the 9 sampling sites consisted in collection of physicochemical parameters (pH, Conductivity, Temperature, Turbidity, OD, ORP, TDS, Salinity, Color, TSS and DOC) of water and metals (As, Cd, Co, Cr, Cu, Ni, Pb and Zn) concentrations in water and sediment of streams located right after the GM site and relate these to indicators of area change (AC and AP). GM sites area range from 121.5 to 0.81 ha and they are ordered in descending order as follows: P5>P8>P1>P6>P4>P3>P7>P9>P2 (Table S7). GM area change from 2015 to 2020 for each site ranged from 2.62% to 1680%, sites which increased their area were P1, P3, P4, P5 and P8 while GM area for sites P2, P6, P7 and P9 decreased. The portion of the GM affected area during the 6-year period that the area of GM sites for 2020 occupied ranged from 1.78% to 68.19%, sites P1, P2 P3, P4, P5, P6 were above 10% percent and sites P7 and P9 were under 10%. These results suggest the points P1, P3, P4, P5 and P6 are having recent activity because they are increasing over time and its actual extent occupies a higher percentage of the total affected area. P6, P7 and P9 show to be reducing its extent and its actual extent is less than 10% of what it has been in the whole 6-year period.

Regarding physicochemical parameters, water temperature and TSS exceed the CCME, TULSMA and EPA normatives, while OD was under the minimum allowed. Sites P4, P5 and P7 were above 28°C, all sites (except P1 and P2) were under 80% of OD and all sites (except P2, P4, P6 and P7) were above 130 mg/L of TSS (Table S7). Conductivity went from 25 to 194.1 µs/cm, turbidity from 10.20 to 1690 NTU, TDS were between 14.95 and 122 mg/L. ORP ranged from 67.3 to 172.7 mV, salinity from 0.006 to 0.090 g/L, color was between 63 and 5250 Pt-Co units and DOC between 1.74 and 8.01 mg/L. Most of these parameters tend to increase due to reduction of vegetation cover, the increment of

erosion, sediment discharges and runoff which are associated with GM activities (Lewis, Garcia-Chevesich, Wildeman, & Sharp, 2020). Also, high turbid waters can affect the photosynthesis of submerged plants, impacting primary productivity and DO production.

Five of eight metals in water were above the maximum allowed limit by CCME, TULSMA and EPA normatives, these were As in site P3, Cd in site P7, Cu in all sites, Pb in all sites but P4 and Zn in all sites (Table S8). Waste from GM is known to contain high Pb, Cu and Cd concentrations, but also other toxic metals like As and Zn making them easily available in the environment (Amoakwah et al., 2020; Appleton, Williams, Orbea, & Carrasco, 2001; Betancourt, Narváez, & Roulet, 2005; Tarras-Wahlber et al., 2000; Wasserman, Campos, Hacon, Farias, & Caires, 2007). Only Cu concentration in P5 sediment was above the national and international normative (Table S9). Enrichment of Cu in stream sediment has been reported before and associated with GM (Obaje, Ogunyele, Adeola, & Akingboye, 2019). Site P5 was the most contaminated site by metals in water and sediment samples, while P4 was the least contaminated site by metals in water and P7 in sediment samples. Sites ordered from the most contaminated by metals in water to the least were P5 > P1 > P3 > P7 > P8 > P2 > P9 > P6 > P4 and in sediment were P5 > P2 > P8 > P4 > P6 > P3 > P9 > P1 > P7. The highest metal concentration detected in water was Zn and in sediment was Cr. The occurrence of metals in decreasing order was Zn > Cu > Pb > Ni > As > Cr > Co > Cd for water and Cr > Zn > Cu > Ni > Co > As > Pb > Cd for sediment samples.

For water samples, Dim1 (PC1) explained 33.7% of data variance and Dim2 (PC2) 20.7%. P2 and P4 were highly correlated with OD; P3 and P1 were correlated with GM area and their change indicators (AC and AP) and metals like Pb and Zn while P6, P7 and P8 were related with physicochemical parameters. Sampling (P1, P2, P3, P4, P5) sites that were geographically closer to each other were found to be in the same cluster for water samples. For sediment samples, PC1 explained 72.7% of data variance and separated the samples mostly by metal concentration while PC2 (17.2% of variance) separated sampling sites by GM area change indicators. P5 was the site mostly associated with metal concentrations while P1 and P3 with AC and AP indicators.

In general, P5 was the most impacted by GM presenting the highest metal contamination in both water and sediment, the biggest area, and also the highest AP value, which means most of the area has been impacted in the last years with a rapid increase, despite it being impacted before 2015. However, more recently exploited sites like P1 and

P3 which had an abrupt growth since 2015 have similar metal contamination in water but a relatively lower metal contamination in sediments. P2, P4, P6 and P8, showed to be increasing but at a lower level than P1, P3 and P5, but showing a higher metal contamination in sediments and a lower metal contamination in water. Those points have a higher dynamic in its position than in its expansion. Otherwise, P7 seems to be reducing but still presenting GM activities near where the collection was done, showing a moderate metal contamination in water with Cd, Cr, Pb, Zn and temperature over the maximum permissible value and DO under the minimum. In P9, the AP value says that in 2020 the GM activities are reduced but metal contamination remains and other consequences like a low DO and the highest TSS value.

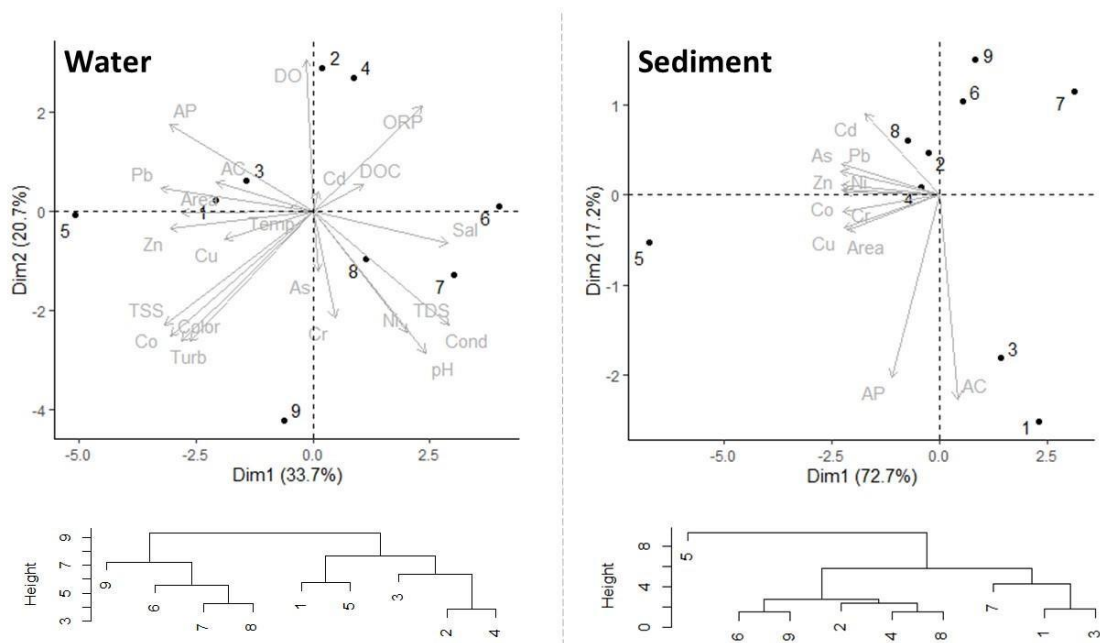


Figure 6. PCA analysis for water and sediment. Dim1 and Dim2 axes are the first two principal components. Results of hierarchical cluster analysis for water and sediment are under its respective PCA plot. Sampling point location area shown in Figure 1 and its coordinates in Table S2.

4. Conclusion

Despite the importance of NRUB and other biodiversity hotspots in the Amazon which are under pressure due to GM activities, their severe consequences on LCLU change and environmental quality have not been addressed yet. We used remote sensing to determine the extent of GM areas from 2015 to 2020 and its relation with LCLU change during this 6-year period. The use of multisource data showed to increase classification accuracy, especially when spectral indices derived from optical image collection are

included. In order to reduce misclassification, the use of other spectral indices, lower resolution and automatization are recommended. LCLU change analysis helped to address the transition of each class determining a high loss of HDV, while GM and other degradative activities gained extent. GM doubled its extent from 0.15% (651 ha in 2015) to 0.30% (1317 ha in 2020) of the total study area and post exploitation landscapes were mainly covered by AZ and LDV. There is no clear association of GM area change from 2015 to 2020 with other variables like gold exploration and production, but it seems to increase with gold price and decrease when ARCOM increased its efforts to control mining in 2018 - 2019.

The combination of GM area change indicators with environmental quality data have made it possible to evaluate the impact of the mining activity in an integrative way, showing that sites with higher increase of land cover and landscape degradation have an effect on water metal contamination and physicochemical parameters like TSS, DO and temperature, while sites with lower increase present a higher occurrence of metals in sediment and a major change of its location than its extent. Finally, sites where GM has reduced its activities showed a reduction in metal contamination but its consequences in physicochemical parameters like low DO and high TSS and turbidity remain long-term. These results are helpful to understand the impacts and dynamics of GM in LCLU change and environmental quality affectation in the period of study, and this integrative approach can be used in future environmental monitoring to avoid difficult access and the danger of mining sites, as well as prioritizing future sampling areas. While remote sensing is not a solution to the wave of illegal and/or environmentally damaging mining, it serves to have an image of the problem and thus readjust the policies or efforts of regulatory government entities. Future monitoring information will be key, because it can be used for long-term environmental management, as well as to know the recovery and rehabilitation of mining areas. These actions are essential to avoid or reduce negative impacts on communities, ecosystems, and water and aquatic resources.

Acknowledgments

This investigation is part of OLS undergraduate thesis and received financial support from the European Union in coordination with the Spanish Cooperation International Agency for Development (AECID), granted to Mariana Velloso Capparelli and Andreu Rico. The author is thankful to the government institutions Ministerio de Ambiente y Agua del Ecuador (MAAE) Dirección Zonal 8, the technician Christian Merino for assistance during

the field trip, Defensoría del Pueblo del Ecuador (DPE) Napo delegation, Policía Nacional del Ecuador for the guard in the trip help. Marcela Cabrera, Carolina Ñacato and Andrea Salgado for their technical support. The author is also thankful to Daniela Alvear, Samantha Vasco, Lady Shiguango, Mariuxi Ramos, Jeniffer Guamangallo and Jakeline Cevallos for their help during the sampling.

Compliance with Ethical Standards

Conflict of interest

The author declares that he has no known competing financial interests or personal relationships that could influence the present investigation.

References

- Adler Miserendino, R., Bergquist, B. A., Adler, S. E., Guimarães, J. R. D., Lees, P. S. J., Niquen, W., ... Veiga, M. M. (2013). Challenges to measuring, monitoring, and addressing the cumulative impacts of artisanal and small-scale gold mining in Ecuador. *Resources Policy*, 38(4), 713–722. <https://doi.org/10.1016/j.resourpol.2013.03.007>
- Agencia de Regulación y Control del Agua (ARCOM). (2018). *Estadística Minera 2018*. Retrieved from <http://www.controlminero.gob.ec/>
- Agencia de Regulación y Control del Agua (ARCOM). (2019, December). ARCOM informa. *Revista Digital ARCOM Informa*, 4–26. Retrieved from www.controlminero.gob.ec
- Alexiades, A. V, Encalada, A. C., Lessmann, J., & Guayasamin, J. M. (2019). Spatial prediction of stream physicochemical parameters for the Napo River Basin, Ecuador. *Journal of Freshwater Ecology*, 34(1), 247–261. <https://doi.org/10.1080/02705060.2018.1542353>
- Amoakwah, E., Ahsan, S., Rahman, M. A., Asamoah, E., Essumang, D. K., Ali, M., & Islam, K. R. (2020). Assessment of Heavy Metal Pollution of Soil-water-vegetative Ecosystems Associated with Artisanal Gold Mining. *Soil and Sediment Contamination*, 29(7), 788–803. <https://doi.org/10.1080/15320383.2020.1777936>
- Anaya, J. A., Gutiérrez-Vélez, V. H., Pacheco-Pascagaza, A. M., Palomino-Ángel, S., Han, N., & Balzter, H. (2020). Drivers of forest loss in a megadiverse hotspot on the Pacific Coast of Colombia. *Remote Sensing*, 12(8), 1–16. <https://doi.org/10.3390/RS12081235>

- APHA. (2018). 2540 solids. In *Standard Methods For the Examination of Water and Wastewater (Vol. 1-0)*. <https://doi.org/10.2105/SMWW.2882.030>
- Appleton, J. D., Williams, T. M., Orbea, H., & Carrasco, M. (2001). Fluvial contamination associated with artisanal gold mining in the Ponce Enríquez, Portovelo-Zaruma and Nambija areas, Ecuador. *Water, Air, and Soil Pollution*, *131*(1–4), 19–39. <https://doi.org/10.1023/A:1011965430757>
- Asner, G. P., Llactayo, W., Tupayachi, R., & Luna, E. R. (2013). Elevated rates of gold mining in the Amazon revealed through high-resolution monitoring. *Proceedings of the National Academy of Sciences of the United States of America*, *110*(46), 18454–18459. <https://doi.org/10.1073/pnas.1318271110>
- Asner, G. P., & Tupayachi, R. (2017). Accelerated losses of protected forests from gold mining in the Peruvian Amazon. *Environmental Research Letters*, *12*(9). <https://doi.org/10.1088/1748-9326/aa7dab>
- Banco Central del Ecuador (BCE). (2017). *Reporte de minería 2017*. Quito-Ecuador.
- Banco Central del Ecuador (BCE). (2020). *Reporte De Minería 2020*. Retrieved from <https://contenido.bce.fin.ec/documentos/Estadisticas/Hidrocarburos/ReporteMinero012020.pdf>
- Barraza, F., Maurice, L., Uzu, G., Becerra, S., López, F., Ochoa-Herrera, V., ... Schreck, E. (2018). Distribution, contents and health risk assessment of metal(loid)s in small-scale farms in the Ecuadorian Amazon: An insight into impacts of oil activities. *Science of the Total Environment*, *622–623*, 106–120. <https://doi.org/10.1016/j.scitotenv.2017.11.246>
- Belgiu, M., & Drăgu, L. (2016). Random forest in remote sensing: A review of applications and future directions. *ISPRS Journal of Photogrammetry and Remote Sensing*, *114*, 24–31. <https://doi.org/10.1016/j.isprsjprs.2016.01.011>
- Betancourt, O., Narváez, A., & Roulet, M. (2005). Small-scale gold mining in the Puyango River basin, southern Ecuador: A study of environmental impacts and human exposures. *EcoHealth*, *2*(4), 323–332. <https://doi.org/10.1007/s10393-005-8462-4>
- Bravo-Medina, C., Marín, H., Marrero-Labrador, P., Ruiz, M. E., Torres-Navarrete, B., Navarrete-Alvarado, H., ... Changoluisa-Vargas, D. (2017). Evaluación de la sustentabilidad mediante indicadores en unidades de producción de la provincia de Napo, Amazonia Ecuatoriana. *Bioagro*, *29*(1), 23–36.

- Brooks, T. M., Mittermeier, R. A., Da Fonseca, G. A. B., Gerlach, J., Hoffmann, M., Lamoreux, J. F., ... Rodrigues, A. S. L. (2006). Global biodiversity conservation priorities. *Science*, *313*(5783), 58–61. <https://doi.org/10.1126/science.1127609>
- Caballero Espejo, J., Messinger, M., Román-Dañobeytia, F., Ascorra, C., Fernandez, L. E., & Silman, M. (2018). Deforestation and forest degradation due to gold mining in the Peruvian Amazon: A 34-year perspective. *Remote Sensing*, *10*(12), 1–17. <https://doi.org/10.3390/rs10121903>
- Canadian Council of Ministers of the Environment (CCME). (2002). *Canadian environmental quality guidelines* (Vol. 2).
- Capolupo, A., Monterisi, C., & Tarantino, E. (2020). Landsat Images Classification Algorithm (LICA) to automatically extract land cover information in Google Earth Engine environment. *Remote Sensing*, *12*(7). <https://doi.org/10.3390/rs12071201>
- Capparelli, M. V., Moulatlet, G. M., Abessa, D. M. de S., Lucas-Solis, O., Rosero, B., Galarza, E., ... Cipriani-Avila, I. (2020). An integrative approach to identify the impacts of multiple metal contamination sources on the Eastern Andean foothills of the Ecuadorian Amazonia. *Science of the Total Environment*, *709*, 136088. <https://doi.org/10.1016/j.scitotenv.2019.136088>
- Carranco, A. (2017). *Breve Resumen Del Contexto Geológico-Minero Regional Del Ecuador*. 19.
- Charou, E., Stefouli, M., Dimitrakopoulos, D., Vasiliou, E., & Mavrantza, O. D. (2010). Using remote sensing to assess impact of mining activities on land and water resources. *Mine Water and the Environment*, *29*(1), 45–52. <https://doi.org/10.1007/s10230-010-0098-0>
- Coulter, L. L., Stow, D. A., Tsai, Y. H., Ibanez, N., Shih, H. chien, Kerr, A., ... Mensah, F. (2016). Classification and assessment of land cover and land use change in southern Ghana using dense stacks of Landsat 7 ETM+ imagery. *Remote Sensing of Environment*, *184*, 396–409. <https://doi.org/10.1016/j.rse.2016.07.016>
- De Alban, J. D. T., Connette, G. M., Oswald, P., & Webb, E. L. (2018). Combined Landsat and L-band SAR data improves land cover classification and change detection in dynamic tropical landscapes. *Remote Sensing*, *10*(2). <https://doi.org/10.3390/rs10020306>
- Delgado-Aguilar, M. J., Konold, W., & Schmitt, C. B. (2017). Community mapping of

- ecosystem services in tropical rainforest of Ecuador. *Ecological Indicators*, 73, 460–471. <https://doi.org/10.1016/j.ecolind.2016.10.020>
- Elmes, A., Ipanaqué, J. G. Y., Rogan, J., Cuba, N., & Bebbington, A. (2014). Mapping licit and illicit mining activity in the Madre de Dios region of Peru. *Remote Sensing Letters*, 5(10), 882–891. <https://doi.org/10.1080/2150704X.2014.973080>
- Frækaland Vangsnes, G. (2018). The meanings of mining: A perspective on the regulation of artisanal and small-scale gold mining in southern Ecuador. *Extractive Industries and Society*, 5(2), 317–326. <https://doi.org/10.1016/j.exis.2018.01.003>
- Galarza, E., Cabrera, M., Espinosa, R., Espitia, E., Moulatlet, G. M., & Capparelli, M. V. (2021). Assessing the Quality of Amazon Aquatic Ecosystems with Multiple Lines of Evidence: The Case of the Northeast Andean Foothills of Ecuador. *Bulletin of Environmental Contamination and Toxicology*, (January). <https://doi.org/10.1007/s00128-020-03089-0>
- Gobierno Autónomo Descentralizado Provincial de Napo (GADP Napo). (2014). La Provincia de Napo. Retrieved July 3, 2020, from Prefectura de Napo website: <http://www.napo.gob.ec/website/>
- Gobierno Autónomo Descentralizado Provincial de Napo (GADP Napo). (2018). *Proyecto de Actualización Plan de Desarrollo y Ordenamiento Territorial de la provincia de Napo 2019 - 2023*.
- Goerner, A., Gloaguen, R., & Makeschin, F. (2007). Monitoring of the Ecuadorian mountain rainforest with remote sensing. *Journal of Applied Remote Sensing*, 1(013527), 1–12. <https://doi.org/10.1117/1.2784111>
- Hurtado Pidal, J. R. (2014). Análisis, modelamiento y simulación espacial del cambio de cobertura del suelo, entre las áreas naturales y las de origen antrópico en la provincia de Napo (Ecuador), para el período 1990-2020 (Universidad Nacional de la Plata). Retrieved from <http://hdl.handle.net/10915/37479>
- Instituto Nacional de Estadística y Censos (INEC). (2010). *Resultados del Censo 2010 de población y vivienda en el Ecuador - Fascículo Provincial Napo*. Retrieved from <http://www.ecuadorencifras.gob.ec/wp-content/descargas/Manu-lateral/Resultados-provinciales/napo.pdf>
- Jiménez-Oyola, S., Escobar Segovia, K., García-Martínez, M. J., Ortega, M., Bolonio, D., García-Garizabal, I., & Salgado, B. (2021). Human health risk assessment for

- exposure to potentially toxic elements in polluted rivers in the ecuadorian amazon. *Water (Switzerland)*, 13(5). <https://doi.org/10.3390/w13050613>
- Keating, P. L. (1997). Mapping vegetation and anthropogenic disturbances in southern Ecuador with remote sensing techniques: implications for park management. *Yearbook - Conference of Latin Americanist Geographers*, 23(1997), 77–90.
- Kumar, L., & Mutanga, O. (2018). Google Earth Engine applications since inception: Usage, trends, and potential. *Remote Sensing*, 10(10), 1–15. <https://doi.org/10.3390/rs10101509>
- Larenas, D., Fierro, V., & Fierro, C. (2017). Minería a Gran Escala: Una Nueva Industria para Ecuador. *Polémika*, (12), 25. Retrieved from <https://www.usfq.edu.ec/publicaciones/polemika/Paginas/revistas/polemika012.aspx>
- Lewis, T. B., Garcia-Chevesich, P. A., Wildeman, T. R., & Sharp, J. O. (2020). Changes in surface water quality from small-scale gold mining operations in the Surinamean rainforest. *Toxicological and Environmental Chemistry*, 102(7–8), 334–355. <https://doi.org/10.1080/02772248.2020.1792908>
- Lobo, F., Costa, M., Novo, E., & Telmer, K. (2016). Distribution of Artisanal and Small-Scale Gold Mining in the Tapajós River Basin (Brazilian Amazon) over the Past 40 Years and Relationship with Water Siltation. *Remote Sensing*, 8(7), 579. <https://doi.org/10.3390/rs8070579>
- Long, E. R., Macdonald, D. D., Smith, S. L., & Calder, F. D. (1995). Incidence of adverse biological effects within ranges of chemical concentrations in marine and estuarine sediments. *Environmental Management*, 19(1), 81–97. <https://doi.org/10.1007/BF02472006>
- Ministerio del Ambiente. (2015). *Acuerdo Ministerial 097-A, de 4 de noviembre de 2015, por el que se reforma el Texto Unificado de Legislación Ambiental Secundaria (TULSMA)*.
- Ministerio del Ambiente de Ecuador. (2015). *Acuerdo N° 97/A - Normas de Calidad Ambiental del Recurso Suelo y Criterios de Remediación para Suelos Contaminados*. Anexo 2, Libro VI de la Calidad Ambiental, del Texto Unificado de la Legislación Secundaria del Ministerio del Ambiente.
- Ministerio del Ambiente y Agua. (2020a). Cobertura de la tierra 2018. Retrieved April 20,

- 2020, from Módulo de Regulación y Control Ambiental (SUIA) website:
<http://ide.ambiente.gob.ec/mapainteractivo/>
- Ministerio del Ambiente y Agua. (2020b). *Línea de base nacional para la Minería Artesanal y en Pequeña Escala de Oro en Ecuador, Conforme la Convención de Minamata sobre Mercurio*. Retrieved from <https://www.ambiente.gob.ec/wp-content/uploads/downloads/2020/06/NAP-Inventario-de-Mercurio-Ecuador.pdf>
- Obaje, S. O., Ogunyele, A. C., Adeola, A. O., & Akingboye, A. S. (2019). Assessment of stream sediments pollution by potentially toxic elements in the active mining area of okpella, edo state, nigeria. *Rudarsko Geolosko Naftni Zbornik*, 34(2), 43–49. <https://doi.org/10.17794/rgn.2019.2.5>
- Perez, G. (2015). *Historia de las ciencias en el ecuador*.
- Pontius, R. G., & Santacruz, A. (2014). Quantity, exchange, and shift components of difference in a square contingency table. *International Journal of Remote Sensing*, 35(21), 7543–7554. <https://doi.org/10.1080/2150704X.2014.969814>
- Potapov, P., Hansen, M. C., Laestadius, L., Turubanova, S., Yaroshenko, A., Thies, C., ... Esipova, E. (2017). The last frontiers of wilderness: Tracking loss of intact forest landscapes from 2000 to 2013. *Science Advances*, 3(1), 1–14. <https://doi.org/10.1126/sciadv.1600821>
- Prefectura de Napo. (2015). *Plan de desarrollo y Ordenamiento Territorial Provincia de Napo*.
- QGIS Development Team. (2021). *QGIS Geographic Information System*. Retrieved from <http://qgis.osgeo.org>
- R Core Team. (2017). *R: A Language and Environment for Statistical Computing*. Retrieved from <https://www.r-project.org/>
- Román-Dañobeytia, F., Huayllani, M., Michi, A., Ibarra, F., Loayza-Muro, R., Vázquez, T., ... García, M. (2015). Reforestation with four native tree species after abandoned gold mining in the Peruvian Amazon. *Ecological Engineering*, 85(December), 39–46. <https://doi.org/10.1016/j.ecoleng.2015.09.075>
- Roy, B. A., Zorrilla, M., Endara, L., Thomas, D. C., Vandegrift, R., Rubenstein, J. M., ... Read, M. (2018). New Mining Concessions Could Severely Decrease Biodiversity and Ecosystem Services in Ecuador. *Tropical Conservation Science*, 11, 194008291878042. <https://doi.org/10.1177/1940082918780427>

- Roy, B., Zorrilla, M., Endara, L., Thomas, D., Vandegrift, R., Rubenstein, J. M., ... Rios-Touma, B. (2018). New mining concessions will severely decrease biodiversity and ecosystem services in Ecuador. *BioRxiv*. <https://doi.org/10.1101/251538>
- Santos, F., Meneses, P., & Hostert, P. (2019). Monitoring long-term forest dynamics with scarce data: a multi-date classification implementation in the Ecuadorian Amazon. *European Journal of Remote Sensing*, 52(sup1), 62–78. <https://doi.org/10.1080/22797254.2018.1533793>
- Secretaría Nacional de Planificación y Desarrollo (SENPLADES). (2015). *Agenda Zonal: Zona 2-Centro Norte. Pichincha*, Napo y Orellana 2013 - 2017 (*excepto el Distrito Metropolitano Quito)* (Vol. 1). Retrieved from www.planificacion.gob.ec
- Song, C. (2004). Cross-sensor calibration between ikonos and landsat ETM+ for spectral mixture analysis. *IEEE Geoscience and Remote Sensing Letters*, 1(4), 272–276. <https://doi.org/10.1109/LGRS.2004.832227>
- Souza, C. M., Shimbo, J. Z., Rosa, M. R., Parente, L. L., Alencar, A. A., Rudorff, B. F. T., ... Azevedo, T. (2020). Reconstructing three decades of land use and land cover changes in brazilian biomes with landsat archive and earth engine. *Remote Sensing*, 12(17). <https://doi.org/10.3390/RS12172735>
- Tarras-Wahlber, N. H., Flachier, A., Fredriksson, G., Lane, S., Lundberg, B., & Sangfors, O. (2000). Environmental impact of small-scale and artisanal gold mining in southern Ecuador: Implications for the setting of environmental standards and for the management of small-scale mining operations. *Ambio*, 29(8), 484–491. <https://doi.org/10.1579/0044-7447-29.8.484>
- Tarras-Wahlberg, N. H., & Lane, S. N. (2003). Suspended sediment yield and metal contamination in a river catchment affected by El Niño events and gold mining activities: The Puyango river basin, southern Ecuador. *Hydrological Processes*, 17(15), 3101–3123. <https://doi.org/10.1002/hyp.1297>
- United States Environmental Protection Agency (US EPA). (1996). *Ecological effects test guidelines*.
- United States Environmental Protection Agency (US EPA). (2014). *Method 200.8: Determination of Trace Elements in Waters and Wastes by Inductively Coupled Plasma-Mass Spectrometry* (Revision 5). Cincinnati, OH.
- Vela-Almeida, D. (2018). Territorial partitions, the production of mining territory and the

- building of a post-neoliberal and plurinational state in Ecuador. *Political Geography*, 62, 126–136. <https://doi.org/10.1016/j.polgeo.2017.10.011>
- Villa-Achupallas, M., Rosado, D., Aguilar, S., & Galindo-Riaño, M. D. (2018). Water quality in the tropical Andes hotspot: The Yacuambi river (southeastern Ecuador). *Science of the Total Environment*, 633, 50–58. <https://doi.org/10.1016/j.scitotenv.2018.03.165>
- Wasserman, J. C., Campos, R. C., Hacon, S. D. S., Farias, R. A., & Caires, S. M. (2007). Mercury in soils and sediments from gold mining liabilities in southern Amazonia. *Quimica Nova*, 30(4), 768–773. <https://doi.org/10.1590/S0100-40422007000400003>
- World Gold Council. (2021). Gold reference prices. Retrieved April 20, 2021, from GOLDHUB website: <https://www.gold.org/goldhub/data/gold-prices>

ANEXOS (Supplementary Materials)

Spatial dynamics of gold mining and its effects on the loss of tropical forests and water resources affectation, applying remote sensors: case of the upper basin of the Napo River, Amazonia, Ecuador.

Table S1. Description of LCLU classes.

LCLU classes	Description	Abbreviation
High density vegetation	Arboreal ecosystem, primary or secondary, regenerated by natural succession, or forest plantations	HDV
Low density vegetation	Shrub or herbaceous vegetation that grows spontaneously or is planted for agricultural or pastoral purposes	LDV
Water of riparian zone	Surface and associated volume of static or moving water	RZ
Anthropic zone	Areas mainly occupied by homes and buildings intended for communities or public services	AZ
Bare soils	Areas generally devoid of vegetation or degraded by human activity	BS
Gold mining	Areas near rivers without vegetation cover where there is a constant removal of soil layers in search of gold	GM
Non observed	Corresponds to areas that could not be classified due to clouds or shadows prevalence	NO
Roads	Civil transport works	It was reclassified into AZ
Beaches	Almost flat expanse of sand or rocks on the banks of a river	It was reclassified into RZ

Table S2. Location of sampling sites.

Sites	Latitud	Longitud
P1	-1.108	-77.860
P2	-1.138	-77.879
P3	-1.137	-77.878
P4	-1.115	-77.868
P5	-1.102	-77.817
P6	-0.987	-77.517
P7	-0.972	-77.497
P8	-1.036	-77.612
P9	-1.050	-77.812

Table S3. Overall accuracy and kappa statistics with different data combinations.

Data combination	Accuracy metrics	
	Overall accuracy	Kappa
Optical	87.55%	0.797
Optical + SAR	87.01%	0.793
Optical + NDVI	87.11%	0.792
Optical + SAR + NDVI	87.39%	0.799
Optical + NDBaI2	87.68%	0.800
Optical + SAR + NDBaI2	87.27%	0.797
Optical + STRedindex	88.27%	0.810
Optical + SAR + STRedindex	87.98%	0.809
Optical + DEM	87.76%	0.801
Optical + DFR	86.90%	0.787
Optical + DEM + DFR	87.76%	0.801
Optical + SAR + NDVI + NDBaI2 + STRedindex + DEM + DFR	88.50%	0.818

Table S4. Accuracy and standard error of user and producer by classes.

Classes	User		Producer	
	Accuracy	Standard Error	Accuracy	Standard Error
HDV	92.81%	0.65%	98.34%	0.25%
LDV	81.92%	1.64%	70.28%	4.16%
RZ	95.12%	3.22%	91.90%	4.13%
AZ	96.25%	2.60%	85.53%	2.61%
BS	74.84%	8.33%	47.71%	7.69%
GM	89.53%	2.72%	77.67%	4.33%
NO	97.62%	2.38%	91.67%	8.33%
Roads	49.94%	3.20%	90.00%	6.83%
Beaches	89.37%	5.05%	95.54%	2.83%

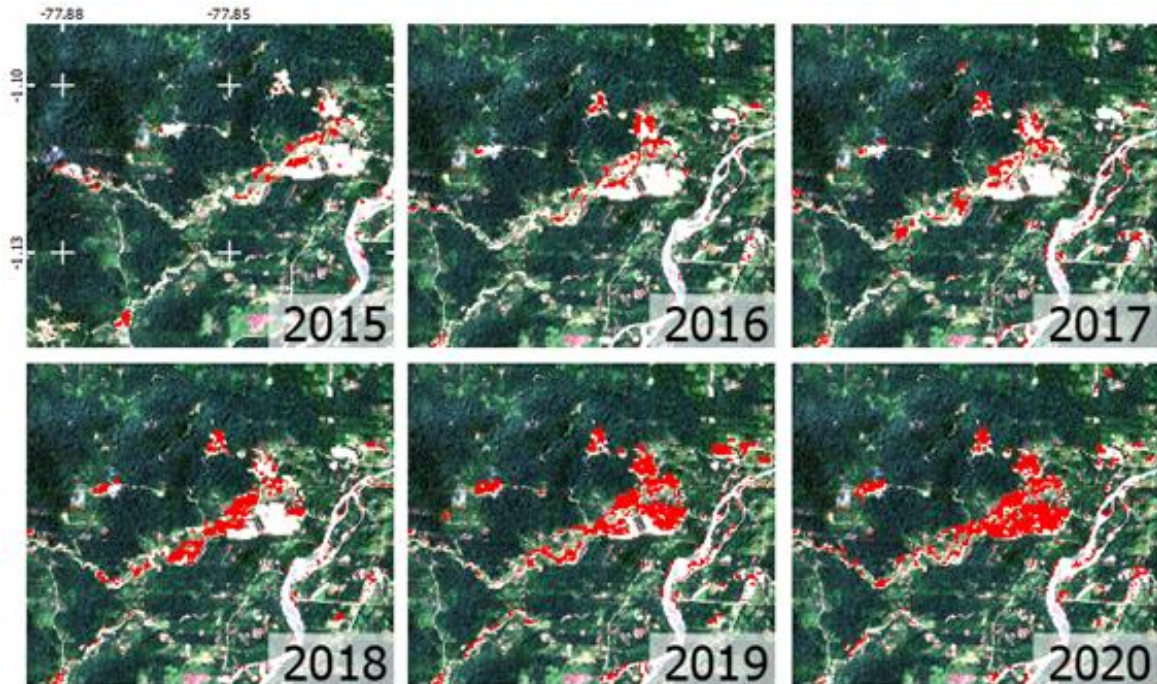


Figure S1. Gold mining land covers evolution from 2015 to 2020 in an example area. The background is a Sentinel-2A image for 2020.

Table S5. Cross-tabulation matrix between 2015 and 2020 classifications.

Category		2020					
		HDV	LDV	RZ	UA	BS	GM
2015	HDV	3803184	439475	14269	9654	44801	2668
	LDV	102243	242685	1396	11114	32219	1657
	RZ	4782	2447	58799	2710	133	1795
	AZ	5089	8083	2322	22833	4984	4495
	BS	16740	36418	1372	7004	12909	1208
	GM	535	1286	690	1795	547	1625

Table S6. Changes between 2015 and 2020 classification per land cover class.

Category	Gain	Persistence	Loss	Quantity	Exchange	Shift
HDV	129389	3803184	510867	381478	258778	0
LDV	487709	242685	148629	339080	290454	6804
RZ	20049	58799	11867	8182	18646	5088
AZ	32277	22833	24973	7304	44546	5400
BS	82684	12909	62742	19942	109246	16238
GM	11823	1625	4853	6970	9706	0
Overall	763931	4142035	763931	381478	365688	16765
(%)	15.57%	84.43%	15.57%	7.78%	7.46%	0.34%

Table S7. Gold mining area change indicators and water physicochemical parameters.

Variable	Sampling sites									Normatives		
	P1	P2	P3	P4	P5	P6	P7	P8	P9	CCME	TULSMA	EPA
Area (ha)	75600	8100	40500	54900	992700	1215000	67500	13500	125100	-	-	-
AC (%)	67.75	25	45.92	41.78	68.19	13.81	3.73	30.09	1.78	-	-	-
AP (%)	1680	52.94	1500	179.41	490.91	74.26	34.88	248.21	2.62	-	-	-
pH	6.91	6.70	6.55	6.67	6.80	7.75	8.06	7.18	7.79	6.5-8.5	6.5-9.0	6.5-9.0
Conductivity (µS/cm)	67.60	25.30	25	53.80	45.80	194.10	187.20	152.30	127.30	500	1000	500
Temperature (°C)	23.30	25.60	30	28.30	29.20	26.60	28.10	26.50	26.70	22.5-27.5	22.0-28.0	22.0-28.0
Turbidity (NTU)	765	10.20	277	24	1457	12.90	28.20	339	1690	-	10	-
OD (% sat)	80.60	81.50	75	76.20	76.60	77.30	76.90	56.50	50.80	>80	>80	>80
ORP (mV)	90.60	147.30	86.30	142	67.30	172.70	86.60	71.30	89.40	-	-	-
TDS (mg/L)	45.50	16.25	14.95	33.20	27.30	122	115	96.20	79.95	500	1000	500
Salinity (g/L)	0.03	0.01	0.01	0.02	0.02	0.09	0.08	0.07	0.01	-	-	-
Color (Pt-Co)	2800	82	375	63	3950	104	78	650	5250	-	-	-
TSS (mg/L)	698.00	3	523.00	19	953.00	58	6	201.00	1024.00	-	130	-
DOC (mg/L)	4.31	1.85	2.40	3.86	3.52	8.01	1.89	1.74	2.39	-	-	-

Table S8. Heavy metals concentration in water (μgL^{-1}) and national and international normatives.

	Sampling sites									CCME		TULSMA	EPA	
	P1	P2	P3	P4	P5	P6	P7	P8	P9	Short Term	Long Term	Freshwater	Acute	Chronic
As	2.169	1.707	6.686	1.379	1.793	3.397	2.759	2.665	3.715	-	5.00	50.00	340.00	150.00
Cd	0.487	0.733	0.176	0.191	0.434	0.176	0.783	0.347	0.266	1.00	0.09	1.00	1.80	0.72
Co	2.145	0.506	1.944	0.451	4.486	0.389	0.610	1.714	4.518	-	-	200.00	-	-
Cr	<2.246	<2.247	2.593	<2.247	<2.247	<2.247	2.780	<2.247	2.306			32.00	-	-
Cu	24.237	6.034	11.957	6.355	11.948	5.644	11.297	10.753	8.435	2.00	-	5.00	-	-
Ni	5.840	3.278	4.329	2.336	1.924	5.818	5.694	4.924	5.751	-	25.00	25.00	470.00	52.00
Pb	6.108	10.538	5.693	0.716	14.500	1.651	1.674	2.420	5.494	-	-	1.00	65.00	2.50
Zn	88.404	30.047	43.411	9.256	144.194	18.943	50.845	50.643	23.301	37.00	7.00	180.00	120.00	120.00

Table S9. Heavy metals concentration in sediment ($\mu\text{g g}^{-1}$) and national and international normatives.

	Sampling sites									CCME		TULSMA
	P1	P2	P3	P4	P5	P6	P7	P8	P9	ISQG-TEL	PEL	Soil
As	0.713	2.002	0.964	1.660	3.633	1.306	0.832	1.585	1.670	5.90	17.00	5.00
Cd	0.013	0.011	0.010	0.021	0.037	0.023	0.020	0.028	0.024	0.60	3.50	0.50
Co	1.698	3.789	2.269	3.511	6.292	2.234	0.895	3.949	2.841	-	-	10.00
Cr	4.755	19.095	11.364	10.120	36.729	9.949	4.321	11.896	7.105	37.30	90.00	20.00
Cu	3.426	4.358	4.142	7.127	10.551	3.662	1.301	5.399	3.973	35.70	197.00	30.00
Ni	2.550	4.886	4.062	5.061	8.715	5.714	2.002	4.336	3.395	-	-	20.00
Pb	0.387	1.201	0.856	1.011	2.169	0.968	0.342	1.141	1.050	35.00	91.30	25.00
Zn	6.090	11.345	6.838	10.570	20.821	9.485	3.516	14.592	8.210	123.00	315.00	60.00